FINITE ELEMENT ANALYSIS OF NON-CRIMP FABRIC LAMINATES UNDER COMPACT TENSION

D. Gouskos[1*], L. Iannucci[2]

[1,2]Department of Aeronautics, Imperial College London, SW7 2AZ London, UK
[1]d.gouskos17@imperial.ac.uk

Keywords: Non-crimp fabric, compact tension, finite element analysis, fracture mechanics, physically-based failure criteria

Abstract
The present work regards the computational analysis of a triaxial [$45^0/0^0/-45^0$] non-crimp fabric (NCF) laminate under compact tension (CT) with the use of finite element methods in Dassault Systèmes Abaqus® 2017 commercial software. Specifically, the scope of this study concerns the calculation of the translaminar fracture toughness of the NCF laminate implementing the physically-based failure criterion LaRC05 [1] as a build-in subroutine in Abaqus. The NCF blanket is consisted of three plies in which the material orientations, 45^0, 0^0, -45^0 are modelled explicitly, while at tow level, fibres, resin and stitches are homogenised with the rule of mixtures. The results of the simulation are compared to existing test results [2] and show good correlation at the pure elastic region, while towards crack onset and propagation mean deviation of approximately 12% is observed.

1. Introduction

Non-Crimped-Fabrics have been under development for some time; they provide certain advantages over traditional pre-impregnated (prepreg) composite materials, mainly a reduction in unit cost and manufacturing cost. Specifically, the non-crimped fabric composites can be produced with an out-of-autoclave manufacturing process; for example, resin transfer moulding (RTM) which is used for woven laminates, is relatively low cost and takes advantage of easy handling of large sheets of the fabric [3].

In terms of strength, NCF do have improved through-thickness properties without significant drop in in-plane performance compared to their conventional prepreg-based counterparts [4]. In addition, NCFs offer new challenging possibilities to designers and manufacturers, given their high degree of tailorability, great deposition rate and improved impact performance [3].

NCFs however, do have a complicated microstructure, hence the application of finite element (FE) methods is necessary to investigate their mechanical performance at all structural levels (from tow level Representative Volume Element [5,6] up to structural component e.g. skin-stiffener configuration [7]). The main disadvantage of the NCFs is the low compressive properties particularly due to fibre waviness (fig. 1). In several research studies [8,9] this structural parameter has been implemented to FE RVE models in order to comprehend the compressive failure mechanisms.

Physically-based failure criteria, as Puck & Schurmann [10] or LaRC05[1] is a promising approach for the description of the structural behaviour of NCFs although they require further refinement in order to be usable for new types of composites with textile reinforcement. Towards this direction Molker et al. [11] presented failure criteria for matrix-dominated failure in NCF-reinforced composites based on LaRC05 criteria and modified to take the orthotropic properties of the NCF into account.

Figure 1. Perpendicular cross-section of UD NCF laminate, presenting fibre waviness [6].

In this work, the translaminar fracture toughness of a triaxial NCF laminate is examined through computational methods. In the past, numerous experimental studies have been carried out [12] but they concerned UD-ply prepreg composites. To the knowledge of the authors, there is not any relevant computational work published for multiaxial NCF under compact tension introducing LaRC05 as constitutive failure model.

2. Materials description & experiment

2.1. Material properties

The material properties have been obtained from literature sources [13,14] and are presented in tables 1 & 2. In particular, Saertex GmbH produced the triaxial NCF composite fabric, which is consisted of Toho Tenax HTS fibres and polyester knitting yarn, infused with Hexcel RTM6 epoxy resin. The nominal thickness of the NCF blanket equals to 0.375mm while the thickness of each fibre tow is 0.125mm. In table 1, subscripts of 11, 22 and 12 denote the longitudinal, transverse and in-plane shear directions respectively. Similarly, in table 2, subscripts of "T" and "C" refer to tension and compression while "S_T" and "S_L" indicate the transverse and longitudinal shear strengths.

Table 1. Nominal membrane properties of the fibre tows in the triaxial NCF blanket [13].

Nominal Membrane Properties			
E_{11} (GPa)	E_{22} (GPa)	G_{12} (GPa)	ν_{12} (-)
130.00	9.00	4.50	0.26

Table 2. Strength values of the fibre tows in the triaxial NCF blanket [14].

Initiation Strengths			
X_T (MPa)	1996.0	Y_C (MPa)	268.0
X_C (MPa)	1531.0	S_T (MPa)	101.0
Y(MPa)	63.9	S_L (MPa)	101.0

2.2. Specimen layup configuration

The layup is expressed at tow level, meaning that the orientations of the individual UD fibre tows within the triaxial NCF blanket are taken into consideration. The exact layup configuration of the specimen is $[(45° / 0° / -45°)_S]_8$.

2.3. Test method

The dimensions of the specimen have been developed by Pinho et al. [12] and are presented in figure 2. Moreover, in figure 2 the critical areas are pointed out where failure is expected to occur during compact tension load. The crack is expected to initiate on the middle of the specimen due to geometric and load symmetry whereas the aft mid part of the specimen should be subjected to local buckling. The applied load (*P*) is expressed as displacement rate equal to 0.5mm/min.

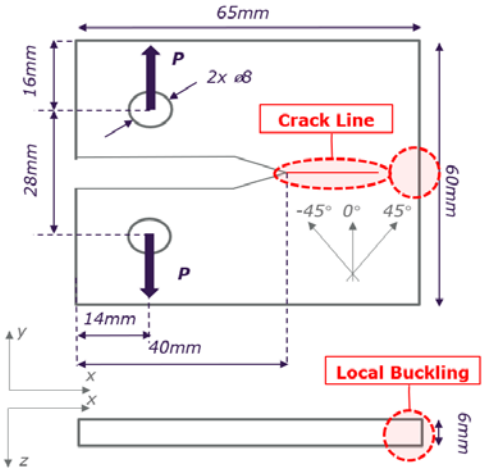

Figure 2. Nominal dimensions of CT specimen and fibre direction.

3. Constitutive Failure Model – LaRC05

LaRC05 which performed very well in the World-Wide Exercise II [15], is going to be the constitutive model for analysing the onset and propagation of fracture. As mentioned in the introduction of this paper, LaRC05 is a pressure-dependent three-dimensional law to predict failure for laminated composites [1]. The failure criteria of LaRC05 in laminated composites can be distinguished between polymer failure, matrix failure, fibre kinking, fibre splitting and fibre tensile failure. Failure occurs when Failure Modes (FM) are equal or greater to 1. Through this model, in-situ strengths are used for matrix failure, while failure propagation takes into consideration the fracture energy associated with each failure mode and the accumulation of cracks in the plies. As it is stated by Pinho et al. [1] this particular 'model is employed to make blind predictions of the triaxial failure envelopes' and in the current research project its application in NCF composites is examined. The current damage propagation model predicts the response of laminates from first ply failure until final laminate failure.

3.1. Polymer failure

In brief, the failure model at ply level, in terms of polymer failure, is based on the Raghava [16] criterion (Eq. 1):

$$FI_P = 3\,(k^2 - (T - C)\,\sigma_h) \,/\, (TC) \tag{1}$$

Where T is the tensile strength of the resin, C is the compressive strength of the resin, σ_h is the hydrostatic stress and k is a variable defined by the principal stresses.

3.2. Matrix failure

Matrix failure criterion is analogous to Raghava's and it is an adaptation of Mohr-Coulomb failure criterion for UD composite plies. The failure index for matrix failure is defined as (Eq. 2):

$$FI_M = (\tau_T / (S^{is}_T - \eta_T \sigma_N))^2 + (\tau_L / (S^{is}_L - \eta_L \sigma_N))^2 + (<\sigma_N>_+ / Y^{is}_T)^2 \quad (2)$$

Where:

- Y^{is}_T, S^{is}_L and S^{is}_T are the in-situ transverse tensile strength, longitudinal shear strength and transverse shear strengths respectively.
- τ_L, τ_T and σ_N are the traction components on the fracture plane of longitudinal shear, transverse shear and normal stress respectively.
- η_T and η_L are the friction coefficients.

For intralaminar matrix failure, the transverse shear strength, S_T, is related to the transverse compressive strength, Y_C, as

$$S_T = Y_C \cos(\alpha_0) (\sin(\alpha_0) + \cos(\alpha_0) / \tan(2\alpha_0)) \quad (3)$$

Where α_0 is the fracture angle for pure transverse compression.

3.3. Fibre kinking & splitting

The criteria proposed for fibre kinking and for splitting use the same failure index equation (Eq. 4), however, the splitting condition is satisfied when $\sigma_1 \geq - X_C/2$, where X_C is the longitudinal compressive strength and σ_1 longitudinal compressive stress. Respectively, the kinking condition is satisfied for $\sigma_1 \leq - X_C/2$.

$$FI_{KINK} = FI_{SPLIT} = (\tau^m_{23} / (S^{is}_T - \eta_T \sigma^m_2))^2 + (\tau^m_{13} / (S^{is}_L - \eta_L \sigma^m_2))^2 + (<\sigma^m_2>_+ / Y^{is}_T)^2 \quad (4)$$

3.4. Fibre tensile failure

Fibre tensile failure is expressed with the maximum stress failure criterion (Eq. 5):

$$FI_{FT} = <\sigma^m_1>_+ / X_T \quad (5)$$

4. Finite element analysis model

LaRC05 is introduced into Dassault System® Abaqus 2017 version in the Standard (Implicit) mode, through two built-in user subroutines “UVARM” and “UDMGINI”. “UVARM” subroutine evaluates the LaRC05 damage criterion and provides output for damage tolerance. It is available both for shell elements (plane stress & continuum) and continuum solid elements. The second subroutine “UDMGINI” evaluates the initiation of the crack and its propagation and is available only for 3D stress states, for three-dimensional stress-displacement continuum elements for which XFEM is supported [17].

Within the frames of this project, a 3D solid model has been examined hence the second subroutine has been implemented with the use of a general purpose linear brick element with reduced integration “C3D8R”.

4.1. Boundary conditions

Boundary conditions are representative of the actual testing constraints. Nodes 1 and 2 as shown in figure 3 are the constraint points of the specimen. For node 1, five out of six degrees of freedom are constrained. Presicely, $U_X = U_Z = UR_X = UR_Y = UR_Z = 0$ but U_Y = 0.5mm/min which is the displacement rate towards positive “y” direction. Similarly, node 2 was constrained in five degrees of freedom, however the unconstrained degree is UR_Z ($UR_Z \neq 0$).

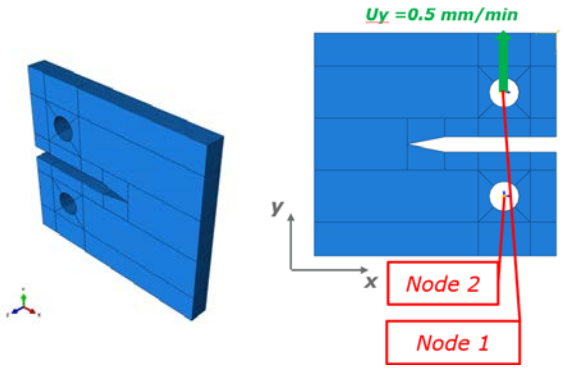

Figure 3. Boundary conditions of the specimen.

4.2. Mesh properties

As it was stated in section 2.2, the plies of the blanket have different material orientations which are explicitly modelled in the finite element analysis (fig. 4). Though, the ply properties are homogenised hence there is no explicit distinction between matric, fibre tows or stitches in the FE modelling. Because of this approach it is assumed that no slippage between the plies occurs as well as no delamination within the NCF blankets.

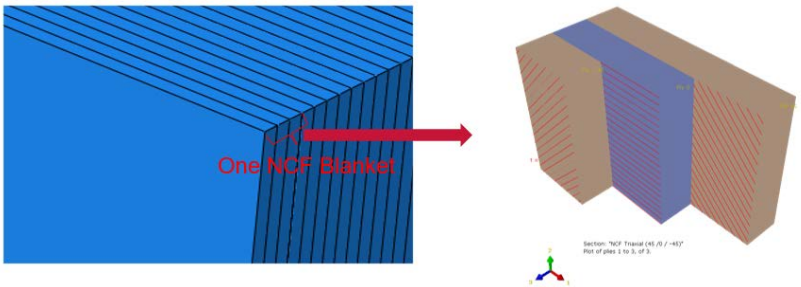

Figure 4. NCF (45^0 / 0^0 / -45^0) blanket modelling.

It has been opted to use a global mesh seed of 1.5mm on the xy-plane but through-the-thickness mesh density equal to ply thickness (i.e. 0.125mm) is applied in order to capture the response of the plies with different material orientations. Moreover, the critical regions for failure onset and propagation have been identified (fig. 5) and increased mesh density of 0.5mm has been applied. On the highlighted middle region of the model (fig. 5) XFEM properties have been introduced since it is a prerequisite for UDMGINI subroutine to capture the failure onset and propagation. An effort has been made to maintain computational time within acceptable limits therefore the increased mesh density and XFEM properties have been assigned to selected partitions of the model. The total number of elements is 103304 elements.

4.3. Input parameters

LaRC05 constitutive model requires the input of certain parameters for proceeding with FE analysis. These parameters are the fracture plane angle for pure compression, α_0, misalignment angle at failure for pure compression, φ_0, friction coefficient, η_T and pressure coefficient, η_L.

Fracture plane angle for pure compression, α_0, varies between 51^0 and 55^0 for Glass & Carbon fibre, the default value of 53^0 has been chosen based on literature sources [18]. Similarly, φ_0 is taken equal to

2.544^0 [18]. Friction coefficient $\eta_{T,}$ is in function of α_0 through formula η_T = - 1/tan($2\alpha_0$), hence for the given data η_T = 0.287. According to [18] η_L = 0.082.

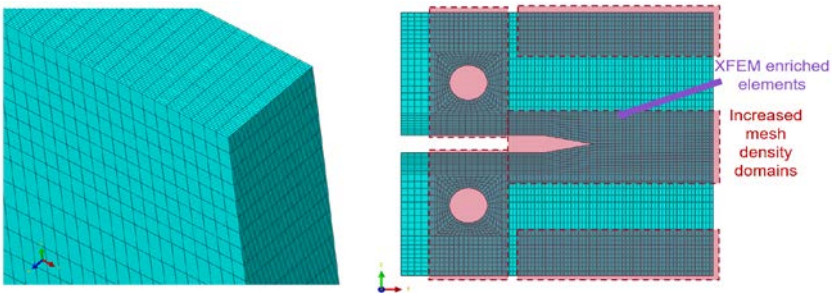

Figure 5. Visualisation of mesh properties and regions with increased mesh density

For crack propagation it is necessary to input the translaminar fracture toughness (G_{IC}) values. These values have been obtained from Gigliottti's et al. experimental study [2] and they refer to failure initiation. A 0º ply has a minimum value of 158 kJ/m^2 while for 45º the respective value is 108 kJ/m^2. With the use of the rule of mixtures [$G_{IC}^{Lam} = t^0_{Lam} / t_{Lam}\, G_{IC}^0 + t^{45}_{Lam} / t_{Lam}\, G_{IC}^{45}$] the NCF laminate fracture toughness is calculated and the value is 128 kJ/m^2.

5. Results

5.1. Load – displacement curves

In figure 6 the applied load in function to displacement is presented and a correlation between the experimental results of Gigliotti et al [2] and the present simulation is made. The initial failure has been considered when the first significant load drop was observed. In the FE simulation the critical load was identified for 11.6 kN while among the test results the maximum respective value was 10.2 kN resulting in deviation of approximately 14%. The ultimate failure is observed at the last load drop which is interpreted as the compressive failure of the buckling region as shown in figure 2.

The failure indices are presented in figure 7a where it is shown that fibre splitting failure (SDV 10) occurs at 45º plies while fibre tensile failure (SDV 11) on 0º plies. Fibre splitting failure happens prior to the fibre tensile failure, while no matrix failure or fibre kinking failure is observed through the respective failure indices (SDV 8 & SDV 9).

5.2. Translaminar fracture toughness

Figure 7b presents the R-curves obtained from the experimental results and the FE simulation. The critical energy release rate (G_{IC}) is calculated with the use of area method as expressed by equation 6.

$$G_{IC} = E/(\alpha\, t) \tag{6}$$

Where: E = total energy used for crack propagation (J), a = crack length (mm) & t = specimen thickness (mm)

The mean value of the critical energy release rate for damage initiation of the tests is 128 kJ/m^2 with a standard deviation of 4% [2] while the FE simulation with LaRC05 shows 132 kJ/m^2 for damage initiation. Regarding damage propagation, as it was stated by Gigliotti et al. [2], no meaningful propagations values could be obtained due to the premature compressive failure of the CT specimens. However, for the FE model, a mean value of 460 kJ/m^2 for crack propagation is observed.

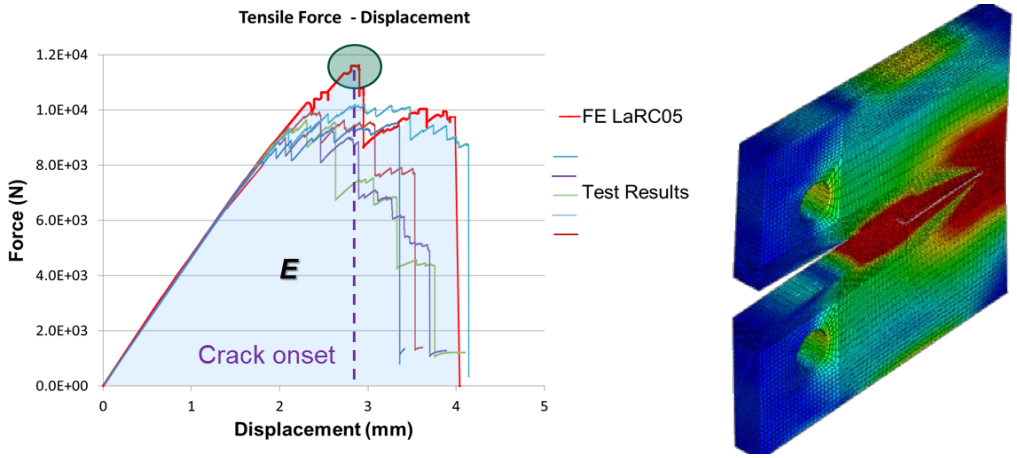

Figure 6. Applied load *(P)* vs. displacement curve for compact tension.

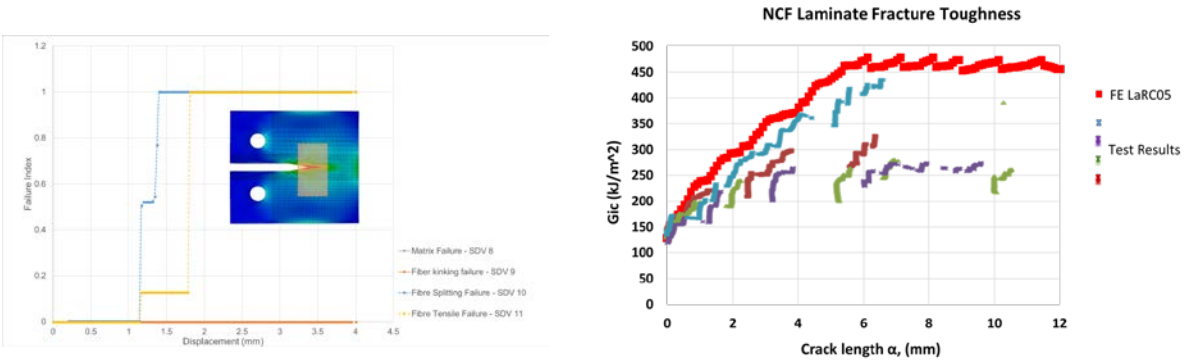

Figure 7. a) Failure indices of the specimen, **b)** R-curves for laminate translaminar fracture toughness.

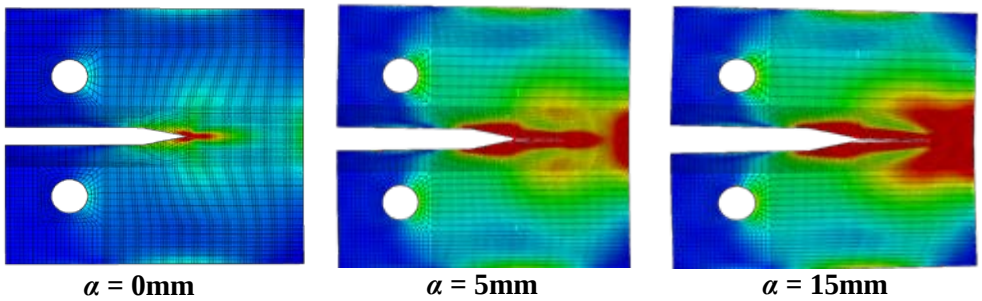

Figure 8. Crack length (α) propagation contour.

6. Conclusions

This conference paper has investigated the simulation of a compact tension test of triaxial NCF with the implementation of LaRC05 as constitutive failure model. The numerical results were correlated with respective experimental [2] and it has been found that there is a promising agreement particularly in the linear elastic region of the load – displacement curve (fig. 6), while a mean deviation of ≈ 12% for the non-linear behaviour is observed. The maximum deviation reached the value of 13.9% at damage onset. Initiation toughness values for both simulation and tests deviate for as little as 4%, however, comparison for the crack propagation data cannot be done because of the premature failure

of the test specimens. The possible reasons which could explain the difference between the results, may involve the existence of defects or flaws of the specimens, not incorporated to the FE model; the effect of stitches was not introduced into the FE model which is the main reason for creating fibre waviness and thus low strength of the NCF, and lastly the fact that no cohesive properties on the interfaces between the NCF blankets have been applied, resulting in the assumption of a perfect bonding among the blankets with zero slippage.

References

[1] Pinho, S., Darvizeh, R., Robinson, P., Schuecker, C., & Camanho, P. Material and structural response of polymer-matrix fibre-reinforced composites. *Journal of Composite Materials*, *46*(19–20), 2313–2341, 2012

[2] Gigliotti, L., & Pinho, S. T. Translaminar fracture toughness of NCF composites with multiaxial blankets. *Materials and Design*, *94*, 410–416, 2016

[3] Lomov, S. V. *Non-crimp fabric composites: Manufacturing, properties and applications*. Woolhead Publishing Series, 2011.

[4] Asp, L. E. Local Models for NCF Composite Materials Mechanical Performance Prediction. *16th International Conference on Composite Materials ICCM-16, Kyoto, Japan*, July 8-13 2007.

[5] Oakeshott, J. L., Iannucci, L., & Robinson, P. Development of a representative unit cell model for bi-axial NCF composites. *Journal of Composite Materials*, *41*(7), 801–835, 2007.

[6] Marklund, E., Asp, L. E., & Olsson, R. Transverse strength of unidirectional non-crimp fabric composites: Multiscale modelling. *Composites Part B: Engineering*, *65*, 47–56, 2014.

[7] Tserpes, K. I., & Labeas, G. N. Mesomechanical analysis of non-crimp fabric composite structural parts. *Composite Structures*, *87*(4), 358–369, 2009.

[8] Ferreira, L. M., Graciani, E., & París, F. Progressive damage study of NCF composites under compressive loading. *16th European Conference on Composite Materials, ECCM-14*, Seville, Spain, June 22–26 2014.

[9] Ferreira, L. M., Graciani, E., & París, F. Three-dimensional finite element study of the behaviour and failure mechanism of non-crimp fabric composites under in-plane compression. *Composite Structures*, *149*, 106–113, 2016

[10] Puck, A., & Schürmann, H. Failure analysis of FRP laminates by means of physically-based phenomenological models. *Composites Science and Technology*, *58*(7), 1045–1067, 1998.

[11] Molker, H., Wilhelmsson, D., Gutkin, R., & Asp, L. E. Orthotropic criteria for transverse failure of non-crimp fabric-reinforced composites. *Journal of Composite Materials*, *50*(18), 2445–2458, 2016

[12] Pinho, S. T., Robinson, P., & Iannucci, L. Fracture toughness of the tensile and compressive fibre failure modes in laminated composites, *Composites Science and Technology*, Volume 66, Issue 13, Pages 2069-2079, 2006.

[13] R. Olsson, Analytical models for impact response and damage growth in sandwich panels, Technical Report CR13-011, Swerea SICOMP, 2013.

[14] T. Block, C. Brauner, M. Zuardy, A. Herrmann, Advanced numerical investigation of the impact behaviour of CFRP foam core sandwich structures, in: Proc. 3rd ECCOMAS Thematic Conference Mech. Resp. Compos., 2011.

[15] Pinho, S. T., Vyas, G. M., & Robinson, P. Material and structural response of polymer-matrix fibre-reinforced composites: Part B. *Journal of Composite Materials*, *47*(6–7), 679–696, 2013.

[16] Raghava R, Caddell RM and Yeh GSY. *The macroscopic yield behaviour of polymers*. Journal Material Science; 8(2): 225–232, 1973.

[17] Dassault System® Abaqus *Manual*, *Simulia Learning Community*. Available from: https://r1132100503382-eu1-3dswym.3dexperience.3ds.com/#home [Accessed 15th May 2018].

[18] Pinho, S. T., Iannucci, L., & Robinson, P. Physically based failure models and criteria for laminated fibre-reinforced composites with emphasis on fibre kinking. Part II: FE implementation. *Composites Part A: Applied Science and Manufacturing*, *37*(5), 766–777, 2006